J. Appl. Comput. Mech., 6(SI) (2020) 1324-1334
DOI: 10.22055/JACM.2020.33464.2230

ISSN: 2383-4536
jacm.scu.ac.ir

Shahid Chamran University of Ahvaz

Journal of Applied and Computational Mechanics

Research Paper

Simultaneous Flow of Three Immiscible Fractional Maxwell Fluids with the Clear and Hoamogeneous Porous Cylindrical Domain

Abdul Rauf, Memoona Naz

Department of Computer Science and Engineering, Air University Multan Campus, Multan, 60000, Pakistan

Received May 02 2020; Revised June 18 2020; Accepted for publication June 18 2020.
Corresponding author: A. Rauf (abdul.rauf@aumc.edu.pk)

Abstract. One-dimensional transient flows of three layers immiscible fractional Maxwell fluids in a cylindrical domain have been investigated in the presence of a porous medium. In the flow, the domain is considered the concentric regions namely one clear region and other two annular regions are filled with a homogeneous porous medium saturated by a generalized Maxwell fluid. The studied problem is based on a mathematical model focused on the fluids with memory described by a constitutive equation with time-fractional Caputo derivative. Analytical solutions to the problem with initial-boundary conditions and interface fluid-fluid conditions are determined by employing the integral transform method (the Laplace transform, the finite Hankel transform and the finite Weber transform). The memory effects and the influence of the porosity coefficient on the fluid motion have been studied. Numerical results and graphical illustrations, obtained with the Mathcad software, have been used to analyze the fluid behavior. The influence of the memory on the fluid motion is significant at the beginning of motion and it is attenuated in time.

Keywords: 3-layered immiscible fluids; Fractional Maxwell fluids; Porous medium; Memory effects; Analytical solutions.

1. Introduction

The study of simultaneous flow of two or more immiscible fluids in porous as well as in clear medium is significant due to its wide applications in science, medical, geophysics, industry, petroleum engineering and hydrogeology [1,49-51]. Various applications include oil recovery, blood flow through capillary vessels, equipment cleaning, biofilms and mucus flow in living cells, removal of carbon dioxide from the atmosphere, groundwater management, crude oil flow through pipelines, bubble generation in microfluidics and bubble trains flow in various complex porous systems.

The flow of two immiscible fluids have many configurations: layers, fingers, encapsulated regimes and drops [40, 52, 53]. One unfavorable thing is that an unknown interface occurs in the domain of our interest while studying of flows of two immiscible fluid like the movement of the interface from one place to another place and even though it may observe sometimes severe deformations, just like a breakup. The linear stability of the viscoelastic two-layered plane Poiseuille and Couette flows have been first studied by Yih [6] with the help of long-wave approach. He observed that both density and viscosity stratification can cause interfacial Kelvin-Helmholtz instability. Later, several researchers have studied the stability/instability of two-layer or multi-layer immiscible fluids flow [2, 4-5]. Herve Le Meur [7] has studied the uniqueness and the existence of the multi-layered Poiseuille/ Couette fluid flow in pipes/channel and observed that interpolated Oldroyd derivative parameter and the viscosity ratios are significant for a unique solution. Kalogirou and Blyth [8] have considered the Couette–Poiseuille flow of the two-layered superposed fluids to discuss stability. The fluid at the lower layer is populated with surfactants and these surfactants get adsorbed on the interface. It has been observed that if the thickness ratio is much higher than the fluid viscosity ratio and if the surfactant is sufficiently soluble, the flow is stable.

The study of the viscoelastic fluid flows in the porous medium is of great interest for many industrial and engineering complex processes such as manufacturing processes of the composite materials, paper and textile coating, optimization of the oil recovery, etc. In [18], authors have worked on incompressible and simultaneous two-layered flow in a porous medium and have derived a set of equations which relates the seepage velocities of the fluid components on continuum level where differentiation make sense. In [19], authors have considered the three-layer simultaneous flow of fully developed fluid in porous media and discussed the characteristics of fluid flow. It has been seen that Darcy's number and the Reynolds number exhibit an important role in the flow velocity.

In [9], Kim et al. have worked on the two-layered immiscible Couette flow with the help of a hybrid method. The flow is between two parallel planes in which the upper plane is moving while the lower plane is kept stationary. It has been found that the viscosity ratio has strong effects on the fluid velocity than the surface energy. In [10], Khan et al have investigated the heat transfer and the fluid velocity of the two-layer immiscible fluid in the presence of pressure type die. The first layer is filled with the inelastic fluid, namely, power-law fluid and the second layer is filled with the viscoelastic liquid (Phan-Thien–Tanner fluids). It has been seen that the fluid velocity and the fluid temperature increase with the increase in the Deborah number. Other interesting results relating to single layer fluid flow [41-48] and the simultaneous flow two or more fluids can be seen in [11–17].

Published online: August 28 2020

Modelling of complex systems with the fractional order differential and integral operators have applications in many fields of science such as geophysics, biology, demography, bioengineering, physics and mathematics; see [20] and the references therein. There exists many fractional differential operators in literature such as Caputo-Fabrizio fractional derivative [20], Riemann-Liouville fractional integral/derivative [21], Caputo fractional derivative [22], and Yang-Srivastava-Machado fractional derivative [23], are some of the examples of the fractional-order differential operators used in viscoelasticity, mass and heat transport processes. Hristov [24] studied the transient space-fractional diffusion with power-law superdiffusivity modelled by the Riemann-Liouville fractional derivative. Ahmad et al. have applied the time-fractional Caputo–Fabrizio derivative to study the two-dimensional advective diffusion process with concentrated source and the short-range memory [25].

In this paper, we have studied the simultaneous flow of the three immiscible fractional Maxwell fluids inside the cylindrical domain. We have divided the cylindrical domain into three concentric simultaneous cylindrical layers. The outer two layers are porous whereas the central layer is clear with no porosity effect. We have considered an unsteady, incompressible and one dimensional fully developed flow which is generated by the movement of the boundary wall.

Moreover, we have considered the linear interfacial fluid-fluid condition between two consecutive layers. To find analytical solutions for velocities we have used the finite Hankel transform and the finite Weber transform in conjunction with the Laplace transformation. The memory effects and the influence of the porosity coefficient on the fluid motion have been studied using numerical simulation and graphical illustrations. The Mathcad software has been employed for this purpose.

2. Basic Constitutive Equations for the Problem

The fundamental expression for the upper convected Maxwell fluid is [29, 41-42]

$$-p\mathbf{I}+\sigma=\tau, \tag{1}$$

with σ being the extra-stress tensor is defined by the relation

$$\sigma+\lambda\left(\frac{\partial\sigma}{\partial t}+v\cdot\nabla\sigma-(\nabla v)^{T}\sigma-\sigma(\nabla v)\right)=\mu A,\ A=\nabla v+(\nabla v)^{T}. \tag{2}$$

In Eqs. (1) and (2) p, $\mathbf{I}$, τ, v, λ, μ, d/dt, ∇v, and the T index are the pressure, the unit tensor, the Cauchy stress tensor, the velocity field, the relaxation time, the fluid viscosity, the material derivative, the velocity gradient tensor, and the transposition operation, respectively.
For the Maxwell fluid upper convected model, the generalized model with time-fractional Caputo derivative is [30,31]

$$\sigma+\lambda^{\alpha}{}^{c}D_{t}^{\alpha}\sigma-\lambda\left[(\nabla v)^{T}\sigma-v\cdot\nabla\sigma+\sigma(\nabla v)\right]=\mu A,\ 0<\alpha\le 1 \tag{3}$$

where the Caputo derivative operator ${}^{c}D_{t}^{\alpha}\sigma(x,y,z,t), 0<\alpha\le 1$ is defined as [32]

$${}^{c}D_{t}^{\alpha}\sigma=\begin{cases}\dfrac{\dot{\sigma}*t^{-\alpha}}{\Gamma(1-\alpha)} & \alpha\in(0,1)\\[2ex] \dot{\sigma}*\delta(t) & \alpha=1\end{cases} \tag{4}$$

$$\dot{\sigma}=\frac{\partial\sigma}{\partial t}, \tag{5}$$

δ-being Dirac's distribution. It is clear from Eqs. (4) and (5) that, for α = 1, the fractional constitutive equation (3) leads to the classical constitutive equation (2) and for λ = 0, Eq. (3) leads to the Newtonian fluid. For the one-dimensional flow with the extra-stress tensor and the velocity field given by

$$\sigma=\sigma(r,t),\mathbf{v}(r,\theta,z,t)=u(r,t)\mathbf{e}_{z},\sigma(r,0)=0,u(r,0)=0, \tag{6}$$

where $\mathbf{e}_z$ represents the unit vector, we get the fractional constitutive relation as

$$(1+\lambda^{\alpha}{}^{c}D_{t}^{\alpha})\delta_{rz}=\mu\frac{\partial u}{\partial r}, \tag{7}$$

Let's consider a porous medium of permeability K saturated by a Maxwell fluid. By analogy with the constitutive equation (7), we can write the following filtration law as [33–35]

$$u=-\frac{K}{\mu\phi}(1+\lambda\frac{\partial}{\partial t})\frac{\partial P}{\partial r}. \tag{8}$$

In Eq. (8), the velocity u, averaged over the pore space, is related to Darcy's velocity by

$$u_{D}=\phi u, \tag{9}$$

where ϕ represents the porosity of the porous medium. In this work, we will consider a generalized form of the filtration law (8), namely [27]

$$(1+\lambda^{\alpha}{}^{c}D_{t}^{\alpha})\frac{\partial P}{\partial r}=-\frac{\mu\phi}{K}u. \tag{10}$$

The local volume-average balance of linear momentum equation is given by [36, 37]

$$\rho\frac{\partial u}{\partial t}=-\frac{\partial P}{\partial r}+\frac{1}{r}\frac{\partial}{\partial r}(r\delta_{rz})+R, \tag{11}$$

where R represents the Darcy's resistance.
It is significant to note that the pressure gradient $\partial p/\partial r$ given by Eq. (10) can be considered as a measure of the same flow resistance in the porous medium bulk [34]. Moreover, Darcy's resistance r in (11) is as well in effect a flow resistance measure caused by the solid matrix, from (10) we have

$$R+\lambda^{\alpha c}D_t^{\alpha}R=-\frac{\mu\varphi}{K}u. \tag{12}$$

Neglecting the pressure gradient $\partial p/\partial r$, Eqs. (7), (11) and (12) lead to the following equation of the linear momentum:

$$(1+\lambda^{\alpha c}D_t^{\alpha})\frac{\partial u}{\partial t}=\frac{\upsilon}{r}\frac{\partial}{\partial r}(r\frac{\partial u}{\partial r})-\frac{\upsilon\phi}{K}u. \tag{13}$$

For a clear fluid (R=0) and in the absence of the pressure gradient $\partial p/\partial r$, Eq. (14) leads to the flow equation

$$(1+\lambda^{\alpha c}D_t^{\alpha})\frac{\partial u}{\partial t}=\frac{\upsilon}{r}\frac{\partial}{\partial r}(r\frac{\partial u}{\partial r}) \tag{14}$$

3. Mathematical Modeling

The flow region is cylindrical

$$\mathfrak{D}=\{(r,\theta,z)\,|\,r\in[0,h],\theta\in[0,2\pi],z\in(-\infty,\infty)\},$$

with z-axis as a flow direction. At the instance t = 0, the boundary cylinder and the fluids inside are at rest. After this instant, the cylinder has motion with velocity $u_3(d,t)=U_0f_1(t)$ along the z-axis (Fig.1). The function $f_1(t)$ is a piece-wise continuous function and $f_1(t)=0$. We considered the flow of 3-layered upper convected Maxwell immiscible fluids with generalized constitutive equations in a domain $r\in[0,h]=[0,h_1]\cup[h_1,h_2]\cup[h_2,h_3]$, inside the cylinder of radius $h:=h_3$. In the domain $r\in[0,h_1]$, Maxwell fluid flows with the density ρ_1, viscosity μ_1, relaxation time $\lambda_1=\mu_1/G_1$, G_1 the elastic modulus, and the velocity $u_1(r,t)$. In the porous annular domains $r\in[h_{i-1},h_i]:h_{i-1}<h_i, i=2,3$, flows a Maxwell fluid with the homogeneous porosity Υ, the density ρ_i, the viscosity μ_i, the relaxation time $\lambda_i=\mu_i/G_i$, G_i the elastic modulus and the velocity $u_i(r,t)$.
The considered fluids are incompressible and immiscible and the stream is unsteady, one dimensional and completely developed. The fluids flow is caused by the movement of the cylinder in the direction of the flow. In view of the suspicions about velocity fields, the continuity equation is indistinguishably fulfilled by all velocities $u_i(r,t), i=1,2,3$ and the equations of the motion take the form [26],

• For clear fluid region, $y\in[0,h_1]$

$$(1+\lambda_1^{\alpha_1 c}D_t^{\alpha_1})\frac{\partial u_1}{\partial t}=\frac{\upsilon_1}{r}\frac{\partial}{\partial r}(r\frac{\partial u_1}{\partial r}), \tag{15}$$

• For the porous second and third annular regions, $y\in[h_{i-1},h_i], i=2,3,$

$$(1+\lambda_i^{\alpha_i c}D_t^{\alpha_i})\frac{\partial u_i}{\partial t}=\frac{\upsilon_i}{r}\frac{\partial}{\partial r}(r\frac{\partial u_i}{\partial t})-\frac{\upsilon_i\varphi}{K}u_i, i=2,3, \tag{16}$$

Along with Eqs. (15) and (16), the following initial and boundary conditions are considered:

$$u_i(r,0)=0,\frac{\partial u_i(r,t)}{\partial t}\,|\,t=0.=0, i=1,2,3. \tag{17}$$

$$\frac{\partial u_1(r,t)}{\partial r}\,|\,r=0=0, u_3(h,t)=U_0f_1(t), U_0>0, \tag{18}$$

$$\begin{gathered}u_1(h_1,t)=u_2(h_1,t),\frac{\partial u_1(r,t)}{\partial r}\Big|_{r=h1}=\frac{\partial u_2(r,t)}{\partial r}\Big|_{r=h_1},\\ u_2(h_2,t)=u_3(h_2,t),\frac{\partial u_2(r,t)}{\partial r}\Big|_{r=h_2}=\frac{\partial u_3(r,t)}{\partial r}\Big|_{r=h_2}.\end{gathered} \tag{19}$$

Consider the following dimensionless parameters

$$\begin{gathered}r^*=\frac{r}{h},t^*=\frac{U_0t}{h},u_i^*=\frac{u_i}{U_0},p^*=\frac{p}{\rho_1U_0^2}.\\ \lambda_i^*=\frac{\lambda_iU_0}{d},\varepsilon_i=\frac{\nu_i}{hU_0},f(t)=f_1\left(\frac{ht}{U_0}\right),d_i=\frac{h_i}{h},h_3=h.\qquad r\in[d_{i-1},d_i]:i=1,2,3.\end{gathered} \tag{20}$$

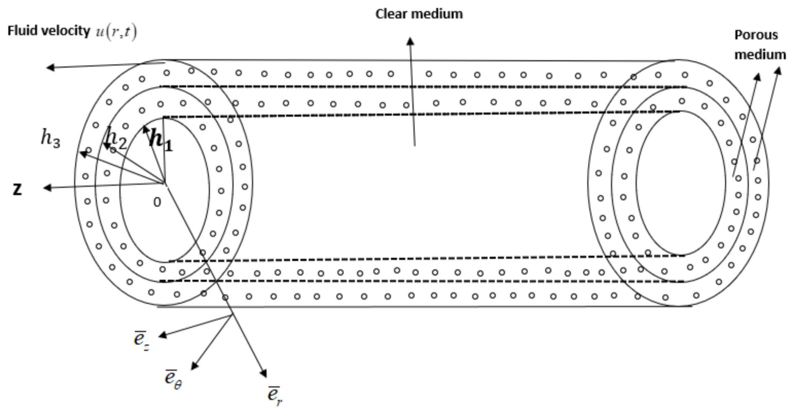

Fig. 1. Geometry of the problem

Eq. (15)-(19) become (neglecting the notation "*")

$$(1+\lambda_1^{\alpha_1}{}^{c}D_t^{\alpha_1})\frac{\partial u_1}{\partial t}=\frac{\varepsilon_1}{r}\frac{\partial}{\partial r}\left(r\frac{\partial u_1}{\partial r}\right), r\in[0,d_1], \tag{21}$$

$$(1+\lambda_i^{\alpha_i}{}^{c}D_t^{\alpha_i})\frac{\partial u_i}{\partial t}=\frac{\varepsilon_i}{r}\frac{\partial}{\partial r}\left(r\frac{\partial u_i}{\partial r}\right)-\Upsilon\varepsilon_i u_i, r\in[d_{i-1},d_i],\ i=2,3, \tag{22}$$

$$u_i(r,0)=0,\frac{\partial u_i(r,t)}{\partial t}|_{t=0}=0, i=1,2,3, \tag{23}$$

$$\frac{\partial u_1(r,t)}{\partial r}|_{r=0}=0, u_3(1,t)=f(t), \tag{24}$$

$$\begin{aligned}u_1(d_1,t)=u_2(d_1,t),\frac{\partial u_1(r,t)}{\partial r}|_{r=d_1}=\frac{\partial u_2(r,t)}{\partial r}|_{r=d_1}\\ u_2(d_2,t)=u_3(d_2,t),\frac{\partial u_2(r,t)}{\partial r}|_{r=d_2}=\frac{\partial u_3(r,t)}{\partial r}|_{r=d_2},\end{aligned} \tag{25}$$

where $\Upsilon=h^2\phi/K$.

4. Analytical Solution

4.1 The clear layer $r\in[0,d_1]$

For the instance i = 1, the fractional governing equation relating the fluid flow in the circular cylinder $r\in[0,d_1]$ along with the suitable initial and boundary conditions can be described as

$$(1+\lambda_1^{\alpha_1}{}^{c}D_t^{\alpha_1})\frac{\partial u_1}{\partial t}=\frac{\varepsilon_1}{r}\frac{\partial}{\partial r}\left(r\frac{\partial u_1}{\partial r}\right), r\in[0,d_1], \tag{26}$$

$$u_1(r,0)=0,\frac{\partial u_1(r,t)}{\partial t}|_{t=0}=0 \tag{27}$$

$$\frac{\partial u_1(r,t)}{\partial r}|_{r=0}=0 \tag{28}$$

To find analytical results from the Eq. (26) with conditions (27), (28) we have applied the Laplace in combination with the finite Hankel transform, namely,

$$\tilde{u}_1(r_{1n},t)=\int_0^{d_1}u_1(r,t)rJ_0(rr_{1n})dr,\ n=1,2,\cdots, \tag{29}$$

the Hankel inverse formulae

$$u_1(r,t)=\frac{2}{d_1^2}\sum_{n=1}^{\infty}\frac{J_0(rr_{1n})}{J_1^2(d_1r_{1n})}\tilde{u}_1(r_{1n},t), \tag{30}$$

where $r_{1n}\geq 0, n=1,2,\cdots,$ satisfy the relation $J_0(d_1x)=0.$ Applying the Laplace transform to Eqs. (26) and (28) and utilizing the initial condition (27), we can write

$$(1+\lambda_1^{\alpha_1}q^{\alpha_1})q\bar{u}_1 = \frac{\varepsilon_1}{r}\frac{\partial}{\partial r}(r\frac{\partial \bar{u}_1}{\partial r}), \tag{31}$$

$$\frac{\partial \bar{u}_1(r,t)}{\partial r}|_{r=0} = 0. \tag{32}$$

Now apply the finite Hankel transform (29) to Eq. (31), we get

$$q\tilde{\tilde{u}}_1 = \frac{\varepsilon_1}{\left(1+\lambda_1^{\alpha_1}q^{\alpha_1}\right)}(d_1\bar{u}_1(d_1,q)r_{1n}J_1(d_1r_{1n}) - r_{1n}^2\tilde{\tilde{u}}_1), \tag{33}$$

Reorganize the Eq. (33) we get

$$\tilde{\tilde{u}}_1(r_{1n},q) = \frac{\varepsilon_1 d_1\bar{u}_1(d_1,q)}{q(1+\lambda_1^{\alpha_1}q^{\alpha_1})+\varepsilon_1 r_{1n}^2} r_{1n}J_1(d_1r_{1n}), \tag{34}$$

To apply the Hankel inverse formulae (30) to Eq. (34), its equivalent form can be written as

$$\tilde{\tilde{u}}_1(r_{1n},q) = \frac{\bar{u}_1(d_1,q)}{d_1r_{1n}^3}(d_1^2r_{1n}^2-4)J_1(d_1r_{1n}) + D_{1n}(q)J_1(d_1r_{1n})\bar{u}_1(d_1,q) \tag{35}$$

where

$$D_{1n}(q) = \frac{4\varepsilon_1 r_{1n}^2 - (d_1^2r_{1n}^2-4)(1+\lambda_1^{\alpha_1}q^{\alpha_1})q}{d_1r_{1n}^3(q(1+\lambda_1^{\alpha_1}q^{\alpha_1})+\varepsilon_1 r_{1n}^2)}. \tag{36}$$

Inverse application of Hankel transform (30) to Eq. (35), we obtain:

$$\bar{u}_1(r,q) = \frac{\bar{u}_1(d_1,q)}{d_1^2}r^2 + \frac{2\bar{u}_1(d_1,q)}{d_1^2}\sum_{n=1}^{\infty}\frac{D_{1n}(q)}{J_1(d_1r_{1n})}J_0(rr_{1n}) \tag{37}$$

In order to obtained the inverse Laplace transforms of the Eq. (37) we write the following supplementary functions for $i=1,2,3$,

$$\begin{aligned}\bar{L}_{i0}(n,q,\Upsilon) &= \frac{1}{q(1+\lambda_i^{\alpha_i}q^{\alpha_i})+\varepsilon_i r_{in}^2+\Upsilon\varepsilon_i} = \frac{q^{-1}}{\lambda_i^{\alpha_i}(q^{\alpha_i}+\lambda_i^{-\alpha_i})\left(1+\dfrac{(\varepsilon_i r_{in}^2+\Upsilon\varepsilon_i)q^{-1}}{\lambda_i^{\alpha_i}(q^{\alpha_i}+\lambda_i^{-\alpha_i})}\right)}\\ &= \frac{1}{\lambda_i^{\alpha_i}}\sum_{j=0}^{\infty}(-1)^j\left(\frac{\varepsilon_i r_{in}^2+\Upsilon\varepsilon_i}{\lambda_i^{\alpha_i}}\right)^j\left[\frac{q^{-j-1}}{(q^{\alpha_i}+\lambda_i^{-\alpha_i})^{j+1}}\right],\end{aligned} \tag{38}$$

and

$$\begin{aligned}\bar{L}_{i2}(n,q,\Upsilon) &:= \lambda_i^{\alpha_i}q(q^{\alpha_i}+\lambda_i^{-\alpha_i})\bar{L}_{i0}(n,q)\\ &= 1+\sum_{j=1}^{\infty}(-1)^j\left(\frac{\varepsilon_i r_{in}^2+\Upsilon\varepsilon_i}{\lambda_i^{\alpha_i}}\right)^j\left[\frac{q^{-j}}{(q^{\alpha_i}+\lambda_i^{-\alpha_i})^j}\right],\end{aligned} \tag{39}$$

Since the generalized G-Lorenzo-Hartley and the Mittag-Leffler functions are defined by [38]

$$G_{a,a_1,a_2}(t,d) = \mathcal{L}^{-1}\left[\frac{q^{a_1}}{(q^a-d)^{a_2}}\right] = \sum_{j=0}^{\infty}\frac{\Gamma(j+a_2)d^jt^{(j+a_2)a-a_1-1}}{j!\Gamma((j+a_2)a-a_1)\Gamma(a_2)}, \tag{40}$$

$$\begin{aligned}&\mathrm{Re}(q)>0,\ \mathrm{Re}(aa_2-a_1)>0,\ |\frac{d}{q^a}|<1,\\ &\mathcal{L}^{-1}\left[\frac{q^{a_i-b_i}}{q^{a_i}-d}\right] = t^{b_i-1}E_{a_i,b_i}(dt^{a_i}),\ a_i,b_i>0,\end{aligned} \tag{41}$$

we have

$$L_{i0}(n,t,\Upsilon) = \sum_{j=0}^{\infty}(-1)^j\frac{\varepsilon_i^j(r_{in}^2+\Upsilon)^j\left[G_{\alpha_i,-j-1,j+1}(t,-\lambda_i^{-\alpha_i})\right]}{(\lambda_i^{\alpha_i})^{j+1}}, \tag{42}$$

and

$$L_{i2}(n,t,\Upsilon) = \delta(t)+\sum_{j=1}^{\infty}(-1)^j\frac{\varepsilon_i^j(r_{in}^2+\Upsilon)^j\left[G_{\alpha_i,-j,j}(t,-\lambda_i^{-\alpha_i})\right]}{(\lambda_i^{\alpha_i})^j}. \tag{43}$$

Applying inverse Laplace transform to Eq. (37), we get the required velocity

$$u_1(r,t)=\frac{u_1(d_1,t)}{d_1^{\,2}}r^2+\frac{2}{d_1^{\,2}}\sum_{n=1}^{\infty}\frac{J_0(rr_{1n})}{J_1(d_1r_{1n})}\left(\frac{4\varepsilon_1}{d_1r_{1n}}u_1(d_1,t)*L_{10}(n,t,0)-\frac{(d_1^{\,2}r_{1n}^2-4)}{d_1r_{1n}^3}u_1(d_1,t)*L_{12}(n,t,0)\right). \tag{44}$$

For the special case, when we consider the single layer case (i.e. $d_1=d_3=1$), our results obtained in Eq. (44) with the condition $u_1(1,t)=Vt$, are equivalent with the results obtained in ([42]; Eq. (24) with $\lambda_r\to 0$).

4.2 For a porous medium (Second and third layers $r\in[d_{i-1},d_i],i=2,3$)

The fractional form of constitutive equations for the simultaneous fluid flow of two immiscible Maxwell fluids in the porous cylindrical annular regions $r\in[d_{i-1},d_i],i=2,3$ can be written as

$$(1+\lambda_i^{\alpha_i c}D_t^{\alpha_i})\frac{\partial u_i}{\partial t}=\frac{\varepsilon_i}{r}\frac{\partial}{\partial r}\left(r\frac{\partial u_i}{\partial r}\right)-\Upsilon\varepsilon_i u_i, i=2,3. \tag{45}$$

the dimensionless initial conditions

$$u_i(r,0)=0,\frac{\partial u_i(r,t)}{\partial r}|_{t=0}=0, i=2,3, \tag{46}$$

the non-dimensional boundary conditions

$$u_3(1,t)=f(t), \tag{47}$$

the dimensionless interface conditions

$$\begin{aligned}u_1(d_1,t)&=u_2(d_1,t),\ \frac{\partial u_1(r,t)}{\partial r}|_{r=d_1}=\frac{\partial u_2(r,t)}{\partial r}|_{r=d_1},\\ u_2(d_2,t)&=u_3(d_2,t),\frac{\partial u_2(r,t)}{\partial r}|_{r=d_2}=\frac{\partial u_3(r,t)}{\partial r}|_{r=d_2}.\end{aligned} \tag{48}$$

To find analytical results of the Eq. (45) with conditions (46), (47) and (48) we have applied the Laplace in combination with the finite Weber transform, namely,

$$\dot{u}_i(r_{in},t)=\int_{d_{i-1}}^{d_i}u_i(r,t)rB_0(r,r_{in})dr, i=2,3, \tag{49}$$

with the inverse Weber transform

$$u_i(r,t)=\frac{\pi^2}{2}\sum_{n=1}^{\infty}\frac{r_{in}^2J_0^2(d_ir_{in})B_0(r,r_{in})}{J_0^2(d_{i-1}r_{in})-J_0^2(d_ir_{in})}\dot{u}_i(r_{in},t), \tag{50}$$

where

$$B_0(r,r_{in})=J_0(rr_{in})Y_0(d_{i-1}r_{in})-J_0(d_{i-1}r_{in})Y_0(rr_{in}). \tag{51}$$

Applying the Laplace transform to Eqs. (45), (47), (48) and utilizing the initial condition (46), we can write

$$\frac{1}{\bar{L}_{i0}(n,q,\Upsilon)}\bar{u}_i(r,q)=\frac{\varepsilon_i}{r}\frac{\partial}{\partial r}[r\ \frac{\partial\bar{u}_i(r,q)}{\partial r}], i=2,3, \tag{52}$$

$$\bar{u}_3(1,q)=\bar{f}(q), \tag{53}$$

$$\begin{aligned}u_1(d_1,q)&=u_2(d_1,q),\ \frac{\partial u_1(r,q)}{\partial r}|_{r=d1}=\frac{\partial u_2(r,q)}{\partial r}|_{r=d_1},\\ u_2(d_2,q)&=u_3(d_2,q),\ \frac{\partial u_2(r,q)}{\partial r}|_{r=d_2}=\frac{\partial u_3(r,q)}{\partial r}|_{r=d_2}.\end{aligned} \tag{54}$$

Now applying the finite Weber transform (49) to Eq. (52), we can write

$$\dot{\bar{u}}_i(r_{in},q)=-\varepsilon_i\bar{L}_{i0}(n,q,\Upsilon)\frac{2}{\pi}\bar{u}_i(d_{i-1},q)+\varepsilon_i\bar{L}_{i0}(n,q,\Upsilon)\frac{2}{\pi}\frac{J_0(d_{i-1}r_{in})}{J_0(d_ir_{in})}\bar{u}_i(d_i,q),\ i=2,3, \tag{55}$$

where the function $\bar{L}_{i0}(n,q,\Upsilon)$ is given by the (38) and with the support of basic properties of Bessel functions and Bessel Wronskian's relation $J_0(\zeta)\ Y_1(\zeta)-J_1(\zeta)\ Y_0(\zeta)=-2/\pi\zeta$, we can write,

$$\int_{d_{i-1}}^{d_i}\frac{\partial}{\partial r}(r\frac{\partial\bar{u}_i(r,q)}{\partial r})B_0(r,r_{in})dr=-r_{in}^2\dot{\bar{u}}_i(r_{in},q)+\frac{2}{\pi}\frac{J_0(d_{i-1}r_{in})}{J_0(d_ir_{in})}\bar{u}_i(d_i,q)-\frac{2}{\pi}\bar{u}_i(d_{i-1},q),\quad n=1,2,\cdots. \tag{56}$$

To apply the inverse Weber transform (50) to Eq. (55), its equivalent form can be written as

$$\dot{\bar{u}}_i(r_{in},q) = \dot{F}_1(r_{in})\bar{u}_i(d_{i-1},q) + \dot{F}_2(r_{in})\bar{u}_i(d_i,q) + S_{in}(q)\bar{u}_i(d_{i-1},q) + Q_{in}(q)\bar{u}_i(d_i,q),\ i \in J_m^{(2)}, \tag{57}$$

where

$$\dot{F}_1(r_{in}) = \frac{1}{d_i^2 - d_{i-1}^2}\Big[\frac{8J_0(d_{i-1}r_{in})}{\pi r_{in}^4 J_0(d_i r_{in})} - \frac{2r_{in}^2(d_i^2 - d_{i-1}^2) + 8}{\pi r_{in}^4}\Big],$$

$$\dot{F}_2(r_{in}) = \frac{1}{d_i^2 - d_{i-1}^2}\Big[\frac{(2r_{in}^2(d_i^2 - d_{i-1}^2) - 8)J_0(d_{i-1}r_{in})}{\pi r_{in}^4 J_0(d_i r_{in})} + \frac{8}{\pi r_{in}^4}\Big],$$

$$S_{in}(q) = -\frac{2\varepsilon_i}{\pi[q(1+\lambda_i^{\alpha_i}q^{\alpha_i}) + \varepsilon_i r_{in}^2] + \Upsilon\varepsilon_i} - \dot{F}_1(r_{in}) = -\frac{2\varepsilon_i}{\pi}\bar{L}_{i0}(n,q,\Upsilon) - \dot{F}_1(r_{in}),$$

$$Q_{in}(q) = \frac{\varepsilon_i}{q(1+\lambda_i^{\alpha_i}q^{\alpha_i}) + \varepsilon_i r_{in}^2 + \Upsilon\varepsilon_i}\frac{2}{\pi}\frac{J_0(d_{i-1}r_{in})}{J_0(d_i r_{in})} - \dot{F}_2(r_{in}) = \frac{2\varepsilon_i}{\pi}\frac{J_0(d_{i-1}r_{in})}{J_0(d_i r_{in})}\bar{L}_{i0}(n,q,\Upsilon) - \dot{F}_2(r_{in}),$$

Applying the inverse Weber transform to Eq. (57) we have

$$\bar{u}_i(r,q) = \frac{d_i^2 - r^2}{d_i^2 - d_{i-1}^2}\bar{u}_i(d_{i-1},q) + \frac{r^2 - d_{i-1}^2}{d_i^2 - d_{i-1}^2}\bar{u}_i(d_i,q) + \frac{\pi^2}{2}\bar{u}_i(d_{i-1},q)\sum_{n=1}^{\infty}\frac{r_{in}^2 J_0^2(d_i r_{in})S_{in}(q)}{J_0^2(d_{i-1}r_{in}) - J_0^2(d_i r_{in})}B_0(r,r_{in}) + \frac{\pi^2}{2}\bar{u}_i(d_i,q)\sum_{n=1}^{\infty}\frac{r_{in}^2 J_0^2(d_i r_{in})Q_{in}(q)}{J_0^2(d_{i-1}r_{in}) - J_0^2(d_i r_{in})}B_0(r,r_{in}) \tag{58}$$

Applying inverse Laplace transform to Eq. (58) we get the velocities $u_i(r,t), i = 2,3$, as

$$u_i(r,t) = \frac{d_i^2 - r^2}{d_i^2 - d_{i-1}^2}u_i(d_{i-1},t) + \frac{r^2 - d_{i-1}^2}{d_i^2 - d_{i-1}^2}u_i(d_i,t) + \frac{\pi^2}{2}\sum_{n=1}^{\infty}\frac{r_{in}^2 J_0^2(d_i r_{in})B_0(r,r_{in})}{J_0^2(d_{i-1}r_{in}) - J_0^2(d_i r_{in})}u_i(d_{i-1},t) * S_{in}(t) + \frac{\pi^2}{2}\sum_{n=1}^{\infty}\frac{r_{in}^2 J_0^2(d_i r_{in})B_0(r,r_{in})}{J_0^2(d_{i-1}r_{in}) - J_0^2(d_i r_{in})}u_i(d_i,t) * Q_{in}(t), i = 2,3, \tag{59}$$

where

$$S_{in}(t) = -\frac{2\varepsilon_i}{\pi}L_{i0}(n,t,\gamma) - \dot{F}_1(r_{in})\delta(t),$$

$$Q_{in}(t) = \frac{2\varepsilon_i}{\pi}\frac{J_0(d_{i-1}r_{in})}{J_0(d_i r_{in})}L_{i0}(n,t,\gamma) - \dot{F}_2(r_{in})\delta(t).$$

4.3 Interface fluid-fluid velocities

Notice that

$$\frac{dB_0(r,r_{in})}{dr} = -r_{in}(J_1(rr_{in})Y_0(d_{i-1}r_{in}) - J_0(d_{i-1}r_{in})Y_1(rr_{r_{in}})) := -r_{in}B_{10}(r,r_{in}) \tag{60}$$

Using the interface conditions (54) in Eqs. (37) and (58) and with the help of Eq. (60), we obtained the following algebraic system

$$\bar{A}(q)\bar{V}(q) = \bar{b}(q), \tag{61}$$

where

$$\bar{A}(q) = \begin{bmatrix}\bar{a}_{11}(q) & \bar{a}_{12}(q)\\ \bar{a}_{21}(q) & \bar{a}_{22}(q)\end{bmatrix},\quad \bar{V}(q) = \begin{pmatrix}\bar{u}_1(d_1,q)\\ \bar{u}_2(d_2,q)\end{pmatrix},\quad \bar{b}(q) = \begin{pmatrix}0\\ \bar{a}(q)\end{pmatrix}, \tag{62}$$

$$\bar{a}_{11} = \bar{T}_{12}(h_1,q) - \bar{T}_{21}(h_1,q),\ \bar{a}_{12} = \bar{T}_{22}(h_1,q), \tag{63}$$

$$\bar{a}_{21} = \bar{T}_{12}(d_2,q),\ \bar{a}_{22} = \bar{T}_{22}(d_2,q) - \bar{T}_{13}(h_2,q), \tag{64}$$

$$\bar{a}(q) = \bar{T}_{23}(d_2,q)\bar{f}(q), \tag{65}$$

$$\bar{T}_{21}(r,q) = \frac{2}{d_1^2}\Big[r - \sum_{n=1}^{\infty}\frac{\bar{B}_{1n}(q)r_{1n}}{J_1(d_1 r_{1n})}J_1(rr_{1n})\Big], \tag{66a}$$

$$\bar{T}_{1i}(r,q) = -\Big[\frac{2r}{d_i^2 - d_{i-1}^2} + \frac{\pi^2}{2}\sum_{n=1}^{\infty}\frac{r_{in}^3 J_0^2(d_i r_{in})S_{in}(q)}{J_0^2(d_{i-1}r_{in}) - J_0^2(d_i r_{in})}B_{10}(r,r_{in})\Big],\ \bar{T}_{2i}(r,q) = \Big[\frac{2r}{d_i^2 - d_{i-1}^2} - \frac{\pi^2}{2}\sum_{n=1}^{\infty}\frac{r_{in}^3 J_0^2(d_i r_{in})Q_{in}(q)}{J_0^2(d_{i-1}r_{in}) - J_0^2(d_i r_{in})}B_{10}(r,r_{in})\Big]\quad i = 2,3. \tag{66b}$$

Solving the linear system (61) we get

$$\bar{u}_1(d_1,q) = -\frac{\bar{a}_{12}(q)\bar{a}(q)}{\bar{a}_{11}(q)\bar{a}_{22}(q) - \bar{a}_{12}(q)\bar{a}_{21}(q)}$$
$$\bar{u}_2(d_2,q) = \frac{\bar{a}_{11}(q)\bar{a}(q)}{\bar{a}_{11}(q)\bar{a}_{22}(q) - \bar{a}_{12}(q)\bar{a}_{21}(q)} \tag{67}$$

Applying the inverse Laplace transform to Eq. (67), we get the interface fluid-fluid velocities $u_1(d_1,t), u_2(d_2,t)$ as

$$\begin{aligned} u_1(d_1,t) &= -a_{12}(t) * a(t) * B(t) \\ u_2(d_2,t) &= -a_{11}(t) * a(t) * B(t) \end{aligned} \tag{68}$$

where B(t) is an auxiliary function such that $[a_{11}(t) * a_{22}(t) - a_{12}(t) * a_{21}(t)] * B(t) = \delta(t)$, $\delta(t)$ is the Dirac delta function, and

$$\begin{aligned} a_{11}((t)) &= T_{12}(h_1,t) - T_{21}(h_1,t), a_{12}(t) = T_{22}(h_1,t), \\ a_{21}(t) &= T_{12}(d_2,t),\ a_{22}(t) = T_{22}(d_2,t) - T_{13}(h_2,t), \end{aligned} \tag{69}$$

$$a(t) = T_{23}(d_2,t) * f(t), \tag{70}$$

$$T_{21}(d_1,t) = \frac{2}{d_1}\left(\delta(t) + \frac{2}{{d_1}^2}\sum_{n=1}^{\infty}\left(4\varepsilon_i L_{10}(n,t,0) - \frac{({d_1}^2 r_{1n}^2 - 4)}{r_{1n}^2} L_{12}(n,t,0)\right)\right), \tag{71}$$

$$\begin{aligned} T_{1i}(d_j,t) &= -\Big[\frac{2d_j}{d_i^2 - d_{i-1}^2} + \frac{\pi^2}{2}\sum_{n=1}^{\infty}\frac{r_{in}^3 J_0^2(d_i r_{in}) S_{in}(t)}{J_0^2(d_{i-1} r_{in}) - J_0^2(d_i r_{in})} B_{10}(d_j, r_{in})\Big], \\ T_{2i}(d_j,t) &= \Big[\frac{2d_j}{d_i^2 - d_{i-1}^2} - \frac{\pi^2}{2}\sum_{n=1}^{\infty}\frac{r_{in} J_0^2(d_i r_{in}) Q_{in}(t)}{J_0^2(d_{i-1} r_{in}) - J_0^2(d_i r_{in})} B_{10}(d_j, r_{in})\Big], \quad i = 2,3, j = 1,2. \end{aligned} \tag{72}$$

5. Numerical Results and Discussions

Simultaneous one-dimensional flow of three layers unsteady immiscible generalized Maxwell fluids between the cylindrical domain have been investigated. In a rectangular coordinate system, we consider a cylinder of radius r = h and at r = 0 the axis of the cylinder is along y-axis. The surface of the cylindrical wall at *r=h* has a translatory motion with velocity $u(h,t) = U_0 f_1(t), U_0 > 0$ being a continuum function of exponential order to infinity and $f_1(0) = 0$.

In this problem, the generalization consists into consideration of the fractional constitutive equation of Maxwell fluids based on Caputo time-fractional derivative. It is clear from the constitutive Eq. (7) that the shear stress σ_{rz} is given by

$$\sigma_{rz}(r,t) = \int_0^t \frac{\mu}{\lambda_\alpha}(t-\varsigma)^{\alpha-1} E_{\alpha,\alpha}\left(-\lambda^{-\alpha}(t-\varsigma)^{\alpha}\right)\frac{\partial u(r,\varsigma)}{\partial\varsigma} d\varsigma, \tag{73}$$

therefore, the history of the velocity gradient influences the shear stress. Such type of flow is the so-called flow with memory.

In the flow channel have been considered three regions, namely the clean region $r \in [0,h_1]$, in which flows a fractional Maxwell fluid and the two regions $r \in [h_{i-1},h_i], i = 2,3$ filled with a porous medium saturated by two different fractional Maxwell fluids. On the solid boundary, the no-slip condition is considered, while at the fluid-fluid interfaces $r = h_1$ and $r = h_2$ the velocities and shear stresses are considered continuous. Using the finite Hankel transform, the finite Weber transform and Laplace transform, the analytical solutions of the problem with initial, boundary and interface conditions have been determined. The flows regions are determined by $d_1 = 0.1$, $d_2 = 0.4$ and $d_3 = 1$.

Numerical results presented in Figs. 2-11 are obtained with the Mathcad software. To study physical features of the fluids motion, it has been considered that in the central core $r \in [0,d_1], d_1 = 0.1$ flows a fractional Maxwell fluid with $\rho_1 = 1000[kg/m^3], \mu_1 = 0.05[Ns/m^2], G_1 = 1.2[N/m^2]$, in the annular section $r \in [d_1,d_2], d_2 = 0.4$ flows a fractional Maxwell fluid categorized by $\rho_2 = 1300[kg/m^3], \mu_2 = 0.2[Ns/m^2], G_2 = 2.4[N/m^2]$ and, in the external layer $r \in [d_2,d_3], d_3 = 1$ flows a fractional Maxwell fluid with $\rho_3 = 1500[kg/m^3], \mu_3 = 0.6[Ns/m^2], G_3 = 5.0[N/m^2]$.

To study the influence of shear stress dumping and the porous medium on the fluid velocity we have analyzed the particular case in which the motion of the cylinder is an oscillation motion with the dimensionless velocity $u(1,t) = 5\text{-}5\cos(t)$. It is observed from Figs. 2 to 10 that the memory effects on the motion of the fluids in the central core is insignificant. The velocity of the fluid from the second layer and the third layer are strongly affected by the memory effects, porosity and due to the interface's interactions. It is observed from Figs. 2 to 10 that the impact of memory effects on the fluids motion in the central core is insignificant. Memory effects, porosity and interfaces connections cause strong influence on the fluid velocities from the second layer and the third layer. The weigh-function $G_{\alpha_i}(t) = t^{\alpha_i - 1}E_{\alpha_i,\alpha_i}(-\lambda_i^{-1}t^{\alpha_i})/\lambda_i$ in Eq. (73) with the increase in the parameter $\alpha_i \in [0,0.7]$ (see Fig., 11), consequently. When the fractional parameters values rise the shear stress values falls and it influences strongly the fluid velocities in second and third layer with porous medium.

Figures 2-10 were illustrated to see the dimensionless variables $\varepsilon_i, i = 1,2,3$ effect on the motion of the fluid. For the numerical computation with characteristic velocities $U_0 \in \{0.100, 0.106, 0.108\}$, we have used the following parameters,

$\in_1 = 1.684\times10^{-3}, \in_2 = 6.734\times10^{-3}, \in_3 = 0.020$ for the Fig. 2-4,

$\in_1 = 1.572\times10^{-3}, \in_2 = 6.289\times10^{-3}, \in_3 = 0.019$ for the Fig. 5-7,

$\in_1 = 1.543\times10^{-3}, \in_2 = 6.173\times10^{-3}, \in_3 = 0.019$ for the Fig. 8-10, separately.

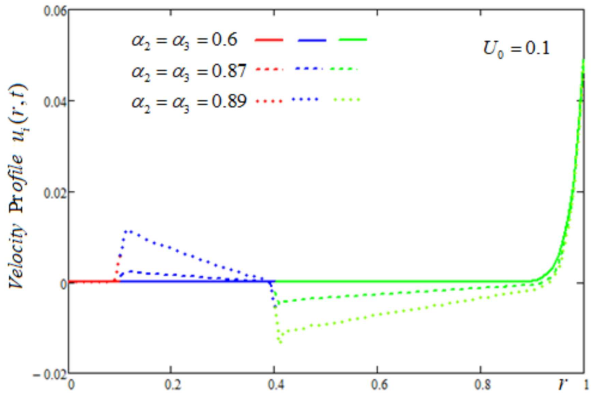

Fig. 2. Velocity profile $u_i(r,t)$ versus r for fractional multi-layers Maxwell fluid at t = 0.14, $t = 0.14, \alpha_1 = 0.2, \Upsilon = 0.3$ and different values of $\alpha_2 = \alpha_3$.

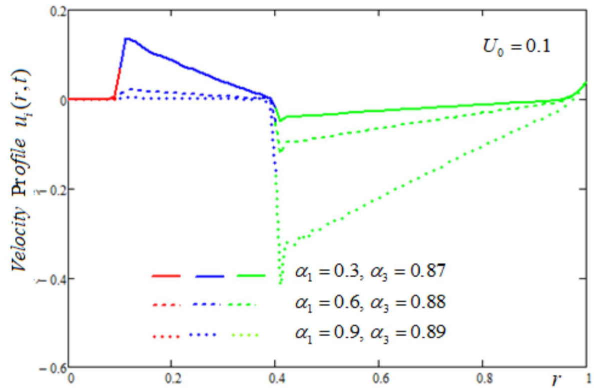

Fig. 3. Velocity profile $u_i(r,t)$ versus r for fractional multi-layers Maxwell fluid at t = 0.125, α_2 = 0.875, ϒ= 0.3 and different values of α_1 and α_3.

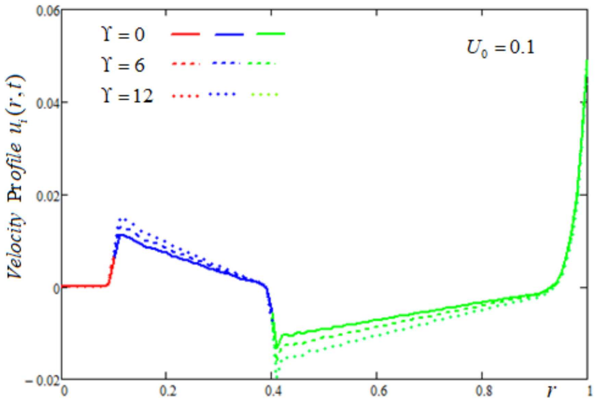

Fig. 4. Velocity profile $u_i(r,t)$ versus r for fractional multi-layers Maxwell fluid at t = 0.14, α_1 = 0.2, $\alpha_2 = \alpha_3$ = 0.89 and different values of ϒ .

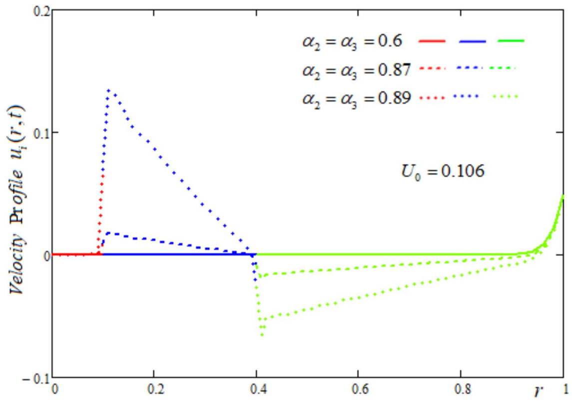

Fig. 5. Velocity profile $u_i(r,t)$ versus r for fractional multi-layers Maxwell fluid at t = 0.14, α_1 = 0.2, ϒ=0.3 and different values of $\alpha_2 = \alpha_3$.

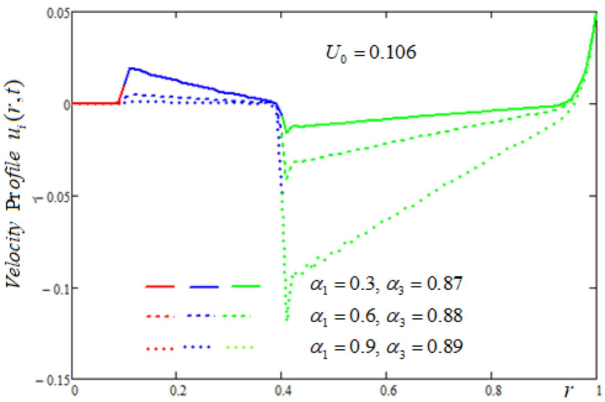

Fig. 6. Velocity profile $u_i(r,t)$ versus r for fractional multi-layers Maxwell fluid at t = 0.125, α_2 = 0.875, ϒ = 0.3 and different values of α_1 and α_3 .

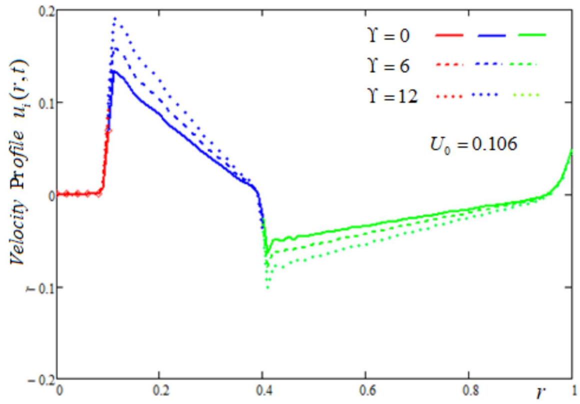

Fig. 7. Velocity profile $u_i(r,t)$ versus r for fractional multi-layers Maxwell fluid at t = 0.14, $\alpha_1 = 0.2, \alpha_2 = \alpha_3 = 0.89$ and different values of ϒ .

From these figures, it can be perceived that the memory effects have a more durable impact when the parameter values $\in_i$, i = 1,2,3 are low. This behavior is more evident for the velocities $u_2(r,t)$ and $u_3(r,t)$ as can been seen in Figs 2-10.

6. Conclusion

Time-dependent simultaneous three-layer of Maxwell fluids immiscible flow in a cylindrical domain have been studied with generic constitutive equations for the shear stress in the presence of porous medium. The mathematical model focused on the fluids with memory specified by a constitutive time-fractional equation with Caputo derivative. An analytic solution have been determined with the help of the finite Hankel transform and the finite Weber transform coupled with the Laplace transformation. The Mathcad software have been used for the graphical representations of the obtained results. The memory effects and the impact of the porosity coefficient on the fluid motion have been considered using numerical simulation and graphical illustrations. It has been observed that the memory effects due to fractional parameters are significant on the fluid motion.

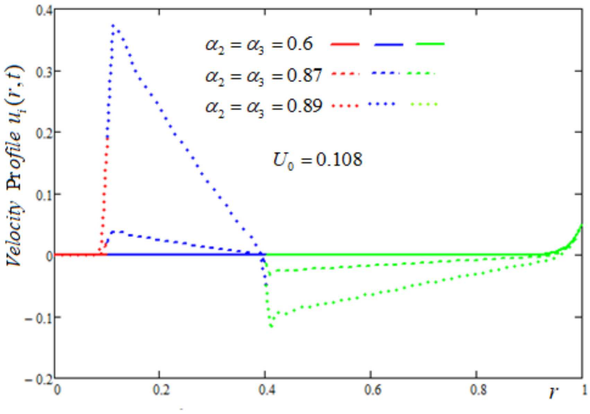

Fig. 8. Velocity profile $u_i(r,t)$ vs. r for fractional multi-layers Maxwell fluid at t = 0.14, $\alpha_1=0.2$, Υ = 0.3 and different values of $\alpha_2=\alpha_3$.

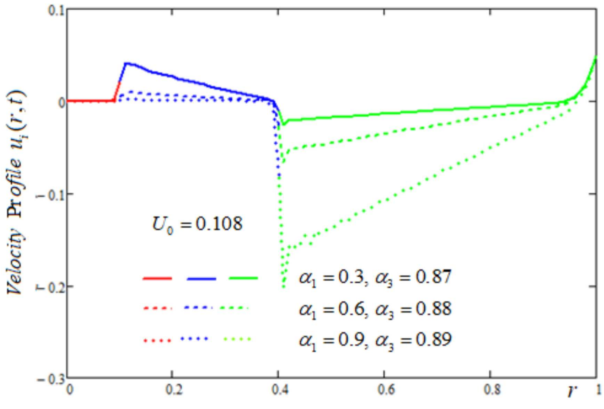

Fig. 9. Velocity profile $u_i(r,t)$ versus r for fractional multi-layers Maxwell fluid at t = 0.125, $\alpha_2=0.875$, Υ = 0.3 and different values of α_2 and α_3.

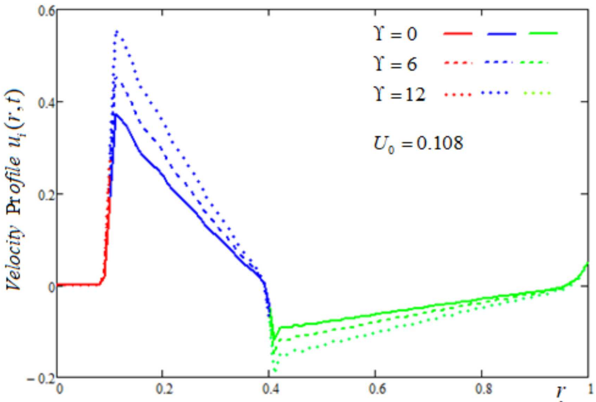

Fig. 10. Velocity profile $u_i(r,t)$ versus r for fractional multi-layers Maxwell fluid at t = 0.14, α_1 = 0.2, $\alpha_2=\alpha_3$ = 0.89 and different values of Υ.

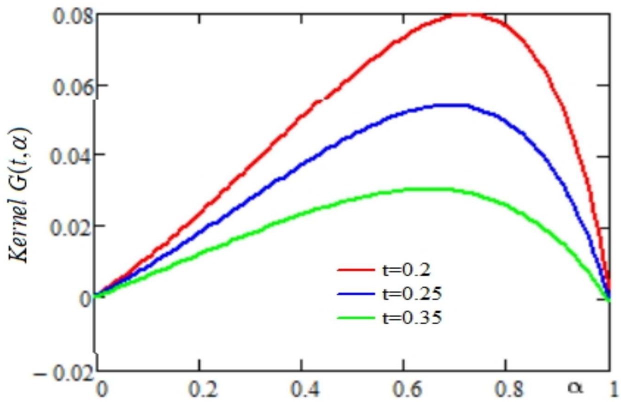

Fig. 11. Profile of the kernel $G(t,\alpha)$.

Authors Contributions

The manuscript was written through the contribution of all authors. All authors discussed the results, reviewed, and approved the final version of the manuscript.

Conflict of Interest

The authors declared no potential conflicts of interest with respect to the research, authorship, and publication of this article.

Funding

The authors received no financial support for the research, authorship, and publication of this article.

References

[1] Satpathi, D.K., Rathish Kumar, B.V. and P. Chandra. Unsteady-state laminar flow of viscoelastic gel and air in a channel: Application to mucus transport in a cough machine simulating trachea. *Mathematical and Computer Modelling* 38(1-2) (2003) 63-75.
[2] Gin, C., and P. Daripa. Stability results for multi-layer radial Hele-Shaw and porous media flows. *Physics of Fluids* 27(1) (2015) 012101.
[3] Nilsen, C. Linear stability analysis of thermoviscous instability in immiscible displacement. *Physical Review E* 97(6) (2018) 063112.
[4] Ward, K., Zoueshtiagh, F. and R. Narayanan. Faraday instability in double-interface fluid layers. *Physical Review Fluids* 4(4) (2019) 043903.
[5] Papaefthymiou, E.S., and D.T. Papageorgiou. Nonlinear stability in three-layer channel flows. *Journal of Fluid Mechanics* 829 (2017) R2.
[6] Yih, C.-S. Instability due to viscosity stratification. *Journal of Fluid Mechanics* 27(2) (1967) 337-352.
[7] Le Meur, H. Non-uniqueness and linear stability of the one-dimensional flow of multiple viscoelastic fluids. *ESAIM: Mathematical Modelling and Numerical Analysis* 31(2) (1997) 185-211.
[8] Kalogirou, A. and M.G. Blyth. The role of soluble surfactants in the linear stability of two-layer flow in a channel. *Journal of Fluid Mechanics* 873 (2019) 18-48.
[9] Kim, Y. et al. Numerical study on the immiscible two-phase flow in a nano-channel using a molecular-continuum hybrid method. *Journal of Mechanical Science and Technology* 33(9) (2019) 4291-4302.
[10] Khan, Z. et al. Flow and heat transfer of two immiscible fluids in double-layer optical fiber coating. *Journal of Coatings Technology and Research* 13(6) (2016) 1055-1063.
[11] Joseph, D.D. and Y.Y. Renardy. Fundamentals of two-fluid dynamics. *Journal of Fluid Mechanics* 282 (1995) 405-405.
[12] Ashraf, S. and J. Phirani. Capillary displacement of viscous liquids in a multi-layered porous medium. *Soft Matter* 15(9) (2019) 2057-2070.
[13] Barannyk, L.L., et al. Nonlinear dynamics and wall touch-up in unstably stratified multilayer flows in horizontal channels under the action of electric fields. *SIAM Journal on Applied Mathematics* 75(1) (2015) 92-113.

[14] Funahashi, H., Kirkland, K.V., Hayashi, K., Hosokawa, S. and Tomiyama, A. Interfacial and wall friction factors of swirling annular flow in a vertical pipe. *Nuclear Engineering and Design* 330 (2018) 97-105.
[15] Papaefthymiou, E.S., and D.T. Papageorgiou. Nonlinear stability in three-layer channel flows. *Journal of Fluid Mechanics* 829 (2017) R2.
[16] Aliyu, M. et al. Interfacial friction in upward annular gas–liquid two-phase flow in pipes. *Experimental Thermal and Fluid Science* 84 (2017) 90-109.
[17] Hisham, M.D., et al. Analytical and semi-analytical solutions to flows of two immiscible Maxwell fluids between moving plates. *Chinese Journal of Physics* 56(6) (2018) 3020-3032.
[18] Hansen, A., et al. Relations between seepage velocities in immiscible, incompressible two-phase flow in porous media. *Transport in Porous Media* 125(3) (2018) 565-587.
[19] Allan, F.M., Hajji, M.A. and M.N. Anwar. The characteristics of fluid flow through multilayer porous media. *Journal of Applied Mechanics* 76(1) (2009) 1-10.
[20] Caputo, M. and M. Fabrizio. A new definition of fractional derivative without singular kernel. *Progress in Fractional Differentiation and Applications* 1(2) (2015) 1-13.
[21] Zhou, Y. Existence and uniqueness of fractional functional differential equations with unbounded delay. *International Journal of Dynamical Systems and Differential Equations* 1(4) (2008) 239-244.
[22] Caputo, M. Linear models of dissipation whose Q is almost frequency independent—II. *Geophysical Journal International* 13(5) (1967) 529-539.
[23] Xiao-Jun, X.J., Srivastava, H.M. and J.T. Machado. A new fractional derivative without singular kernel. *Thermal Science* 20(2) (2016) 753-756.
[24] Hristov, J. Transient space-fractional diffusion with a power-law superdiffusivity: approximate integral-balance approach. *Fundamenta Informaticae* 151(1-4) (2017) 371-388.
[25] Ahmed, N., Shah, N.A. and D. Vieru. Two-Dimensional Advection–Diffusion Process with Memory and Concentrated Source. *Symmetry* 11(7) (2019) 879.
[26] Brechet, Y. and Z. Neda. On the circular hydraulic jump. *American Journal of Physics* 67(8) (1999) 723-731.
[27] Govindarajan, R. Effect of miscibility on the linear instability of two-fluid channel flow. *International Journal of Multiphase Flow* 30(10) (2004) 1177-1192.
[28] Russell, T.W.F., and M.E. Charles. The effect of the less viscous liquid in the laminar flow of two immiscible liquids. *The Canadian Journal of Chemical Engineering* 37(1) (1959) 18-24.
[29] Málek, J., Nečas, J. and M. Růžička. On the non-Newtonian incompressible fluids. *Mathematical Models and Methods in Applied Sciences* 3(1) (1993) 35-63.
[30] Friedrich, C.H.R. Relaxation and retardation functions of the Maxwell model with fractional derivatives. *Rheologica Acta* 30(2) (1991) 151-158.
[31] Hristov, J. Response functions in linear viscoelastic constitutive equations and related fractional operators. *Mathematical Modelling of Natural Phenomena* 14(3) (2019) 305.
[32] Caputo, M. Linear models of dissipation whose Q is almost frequency independent—II. *Geophysical Journal International* 13(5) (1967) 529-539.
[33] Alishaev, M.G. and A.K. Mirzadjanzade. For the calculation of delay phenomenon in filtration theory. *Izvestiya Vysshikh Uchebnykh Zavedeniy. Neft'i Gaz* 6 (1975) 71-78.
[34] Khuzhayorov, B., Auriault, J.-L. and P. Royer. Derivation of macroscopic filtration law for transient linear viscoelastic fluid flow in porous media. *International Journal of Engineering Science* 38(5) (2000) 487-504.
[35] Nield, D.A. Modelling fluid flow and heat transfer in a saturated porous medium. *Advances in Decision Sciences* 4(2) (2000) 165-173.
[36] Xue, C. and J. Nie. Exact solutions of Rayleigh-Stokes problem for heated generalized Maxwell fluid in a porous half-space. *Mathematical Problems in Engineering* 2008 (2008) 641431.
[37] Vafai, K. and C.L. Tien. Boundary and inertia effects on flow and heat transfer in porous media. *International Journal of Heat and Mass Transfer* 24(2) (1981) 195-203.
[38] Lorenzo, C.F. and T.T. Hartley. Generalized functions for the fractional calculus. 1999.
[39] Arshad, M., Choi, J., Mubeen, S., Nisar, K.S. and G. Rahman, A new extension of the Mittag-Lefler function, Commun. *Korean Math. Soc.* 33(2) (2018) 549-560.
[40] Joseph, D.D., Bai, R., Chen, K.P. and Y.Y. Renardy. Core-annular flows. *Annual Review of Fluid Mechanics* 29(1) (1997) 65-90.
[41] Hayat, T., Abbas, Z. and M. Sajid. Series solution for the upper-convected Maxwell fluid over a porous stretching plate. *Physics Letters A* 358(5-6) (2006) 396-403.
[42] Fetecau, C., et al. Some exact solutions for the helical flow of a generalized Oldroyd-B fluid in a circular cylinder. *Computers & Mathematics with Applications* 56(12) (2008) 3096-3108.
[43] Hsiao, K.-L. To promote radiation electrical MHD activation energy thermal extrusion manufacturing system efficiency by using Carreau-Nanofluid with parameters control method. *Energy* 130 (2017) 486-499.
[44] Hsiao, K.-L. Combined electrical MHD heat transfer thermal extrusion system using Maxwell fluid with radiative and viscous dissipation effects. *Applied Thermal Engineering* 112 (2017) 1281-1288.
[45] Hsiao, K.-L. Micropolar nanofluid flow with MHD and viscous dissipation effects towards a stretching sheet with multimedia feature. *International Journal of Heat and Mass Transfer* 112 (2017) 983-990.
[46] Farooq, U., et al. MHD flow of Maxwell fluid with nanomaterials due to an exponentially stretching surface. *Scientific Reports* 9(1) (2019) 1-11.
[47] Khan, I., Shah, N.A. and L.C.C. Dennis. A scientific report on heat transfer analysis in mixed convection flow of Maxwell fluid over an oscillating vertical plate. *Scientific Reports* 7(1) (2017) 1-11.
[48] Rauf, A. An Analytical and Semi-analytical Study of the Oscillating Flow of Generalized Burgers' Fluid through a Circular Porous Medium. *Journal of Applied and Computational Mechanics* 5(5) (2019) 827-839.
[49] Bear, J. *Dynamics of fluids in porous media*. Courier Corporation, 2013.
[50] Dullien, F.A. *Porous media: fluid transport and pore structure*. Academic press, 2012.
[51] Lake, L.W. *Enhanced Oil Recovery,* Prentice Hall, Englewood Cliffs. 1989.
[52] Joseph, D.D. and Y. Renardy. *Fundamentals of Two-Fluid Dynamics, Part I*, Springer-Verlag, New York, 1993.
[53] Joseph, D.D. and Y. Renardy. *Fundamentals of Two-Fluid Dynamics, Part II*, Springer-Verlag, New York, 1993.

ORCID iD

Abdul Rauf https://orcid.org/0000-0001-8173-9496
Memoona Naz https://orcid.org/0000-0002-9290-4634

How to cite this article: Rauf A., Naz M. Simultaneous Flow of Three Immiscible Fractional Maxwell Fluids with the Clear and Homogeneous Porous Cylindrical Domain, *J. Appl. Comput. Mech.*, 6(SI), 2020, 1324–1334.
https://doi.org/10.22055/JACM.2020.33464.2230